

## Dominance of low- $\ell$ component in weakly bound deformed single-neutron orbits

Ikuko Hamamoto

*Division of Mathematical Physics, Lund Institute of Technology at the University of Lund, Lund, Sweden  
and The Niels Bohr Institute, Blegdamsvej 17, Copenhagen Ø, DK-2100, Denmark*

(Received 24 February 2004; published 30 April 2004)

Calculating single-particle (Nilsson) levels in axially symmetric quadrupole-deformed potentials in coordinate space, the structure of weakly bound neutron orbits is studied in the absence of pair correlation. It is shown that in the wave functions of  $\Omega^\pi=1/2^+$  orbits, where  $\Omega$  expresses the projection of the particle angular momentum along the symmetry axis, the  $\ell=0$  ( $s_{1/2}$ ) component becomes overwhelmingly dominant as the binding energy of the orbits approaches zero, irrespective of the size of the deformation and the kind of Nilsson orbits. Consequently, all  $\Omega^\pi=1/2^+$  levels become practically unavailable for both deformation and many-body pair correlation, when the levels approach continuum or lie in the continuum.

DOI: 10.1103/PhysRevC.69.041306

PACS number(s): 21.60.Ev, 21.10.Pc, 21.60.Jz

The physics of nuclei far from the line of  $\beta$  stability, especially close to the neutron drip line, which has been developed for the last years together with the experiments using radioactive nuclear ion beams, issues an intensive challenge to the conventional theory of nuclear structure. A characteristic feature unique to the weakly bound neutron systems is the importance of the coupling to the nearby continuum of unbound states, as well as the impressive role played by weakly bound neutrons with low orbital angular momenta  $\ell$ . A typical phenomenon is the observed change of magic numbers in very light neutron-rich nuclei [1,2] from those known in  $\beta$  stable nuclei. The change can be understood from the difference in the properties of small  $\ell$  neutrons from those of weakly bound large  $\ell$  neutrons, of which the wave functions stay mostly inside the nuclear potential. Weakly bound small- $\ell$  neutrons have an appreciable probability to be outside of the core nucleus and are thereby insensitive to the strength of the potential provided by the well-bound nucleons in the system. As seen in the shell-structure change, the competition between pairing and shape deformation, which has been a central issue in the many-body problem of  $\beta$  stable nuclei [3], is expected to be a fundamentally important theme also in the study of nuclear structure far from the stability line [4]. In neutron drip line nuclei the presence of loosely bound neutrons as well as the very neutron rich environment near the nuclear surface opens new interesting aspects in this competition, which have not yet been well studied.

In Ref. [5] the pair correlation in spherical nuclei close to the neutron drip line, especially the unique role played by weakly bound low  $\ell$  neutrons, was studied by solving the Hartree-Fock-Bogoliubov equation in a simplified model in coordinate space with the correct asymptotic boundary conditions [6–8]. It was shown that for a given bound system the occupation probability of the lower  $\ell$  levels of the Hartree-Fock (HF) potential decreases considerably when the binding energy of the HF one-particle level becomes small, and those orbits soon become almost unavailable for the pair correlation of the many-body system. It was concluded in Ref. [5] that the unavailability of those lower  $\ell$  orbits would be much more serious in deformed nuclei, since the components of lower  $\ell$  orbits spread in essence over all Nilsson orbits with

smaller  $\Omega$  values. In textbooks [3,9] we learn that the Nilsson orbits can be classified in terms of asymptotic quantum numbers  $[Nn_z\Lambda\Omega]$ , where  $\Omega$  is a good quantum number. Other three quantum numbers  $[Nn_z\Lambda]$  would become approximately good quantum-numbers for larger deformation where the effect of axially symmetric quadrupole deformation dominates over the spin-orbit splitting. Indeed, various kinds of experimental data on deformed nuclei close to the  $\beta$  stability line have been very successfully analyzed in terms of the asymptotic quantum numbers [3]. The asymptotic quantum numbers are derived based on the axially symmetric quadrupole-deformed harmonic-oscillator plus spin-orbit potentials, which can be appropriate for analyzing the properties of well-bound  $\beta$  stable nuclei.

In the present paper we study the structure of one-particle orbits in axially symmetric quadrupole-deformed Woods-Saxon plus spin-orbit potentials, solving the Schrödinger equation in coordinate space with the correct asymptotic boundary conditions. We focus our attention on the structure of weakly bound neutron orbits in deformed finite-well potentials.

In order to study the behavior of weakly bound orbits, it is absolutely necessary to use a realistic finite-well potential. For simplicity, we use the Woods-Saxon potential as a replacement of the HF potential and include the deformed part of the Woods-Saxon potential. Our axially symmetric quadrupole-deformed potential consists of the following three parts:

$$V(r) = V_{WS} f(r),$$

$$V_{coupl}(\vec{r}) = -\beta k(r) Y_{20}(\hat{r}),$$

$$V_{so}(r) = -V_{WS} v \left( \frac{\Lambda}{2} \right)^2 \frac{1}{r} \frac{df(r)}{dr} (\vec{\sigma} \cdot \vec{\ell}), \quad (1)$$

where  $\Lambda$  is the reduced Compton wavelength of nucleon  $\hbar/m_r c$ ,

$$f(r) = \frac{1}{1 + \exp\left(\frac{r-R}{a}\right)} \quad (2)$$

and

$$k(r) = RV_{WS} \frac{df(r)}{dr}. \quad (3)$$

We fix the parameters to be  $a=0.67$  fm,  $V_{WS}=-51$  MeV, and  $v=32$ , which are the standard parameters used in  $\beta$  stable nuclei [10]. The nuclear radius  $R$  is varied so as to vary the strength of our one-body potential. Or, equivalently, we vary the mass number  $A$  of the system with  $R=r_0A^{-1/3}$  where  $r_0=1.27$  fm is used. In the expression (1) we have included only the lowest-order term in deformation parameter  $\beta$  of the deformed Woods-Saxon potential. This is an approximation, however, for our present purpose to illustrate the unique behavior of weakly bound low- $\ell$  neutrons the simple form of the deformed potential is sufficient. We write the single-particle wave function as

$$\Psi_m(\vec{r}) = \frac{1}{r} \sum_{\ell j} R_{\ell jm}(r) \mathbf{Y}_{\ell jm}(\hat{r}), \quad (4)$$

which satisfies

$$H \Psi_m = \varepsilon_m \Psi_m. \quad (5)$$

The coupled equation for the radial wave function is written as

$$\begin{aligned} & \left( \frac{d^2}{dr^2} - \frac{\ell(\ell+1)}{r^2} + \frac{2m}{\hbar^2} [\varepsilon_m - V(r) - V_{so}(r)] \right) R_{\ell jm}(r) \\ &= \frac{2m}{\hbar^2} \sum_{\ell' j'} \langle \mathbf{Y}_{\ell jm} | V_{coupl} | \mathbf{Y}_{\ell' j' m} \rangle R_{\ell' j' m}(r), \end{aligned} \quad (6)$$

where

$$\begin{aligned} \langle \mathbf{Y}_{\ell jm} | V_{coupl} | \mathbf{Y}_{\ell' j' m} \rangle &= -\beta k(r) \langle \mathbf{Y}_{\ell jm} | Y_{20}(\hat{r}) | \mathbf{Y}_{\ell' j' m} \rangle \\ &= -\beta k(r) (-1)^{m-1/2} \sqrt{\frac{(2j+1)(2j'+1)}{20\pi}} \\ &\quad \times C(j, j', 2; m, -m, 0) \\ &\quad \times C(j, j', 2; \frac{1}{2}, -\frac{1}{2}, 0). \end{aligned} \quad (7)$$

The eigenvalue  $\varepsilon_m (< 0)$  of the coupled equations (6) for a given value of  $m$ , which is equivalent to  $\Omega$  in the usual notation of asymptotic quantum numbers  $[Nn_z\Lambda\Omega]$ , is obtained by solving the equations in coordinate space for given values of  $\beta$  and  $R$ , with the asymptotic behavior of  $R_{\ell jm}(r)$  for  $r \rightarrow \infty$ ,

$$R_{\ell jm} \propto r h_\ell(\alpha r), \quad (8)$$

where  $h_\ell(-iz) \equiv j_\ell(z) + in_\ell(z)$ , in which  $j_\ell$  and  $n_\ell$  are spherical Bessel and Neumann functions, respectively, and

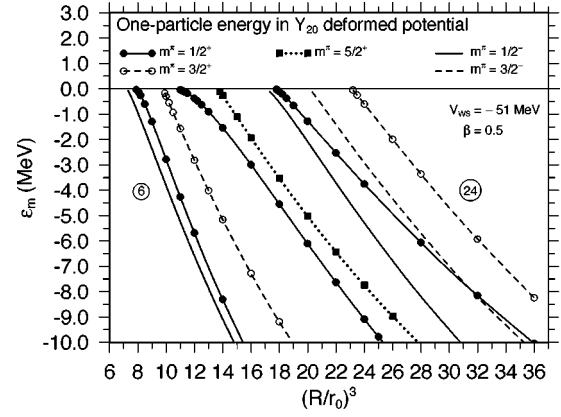


FIG. 1. Neutron energy levels in axially symmetric quadrupole-deformed Woods-Saxon potential as a function of the potential strength. The radius of the Woods-Saxon potential is expressed by  $R$ , while  $r_0=1.27$  fm is used. The asymptotic quantum numbers  $[Nn_z\Lambda\Omega]$  assigned traditionally to these levels are  $[101\ 1/2]$ ,  $[220\ 1/2]$ ,  $[211\ 3/2]$ ,  $[211\ 1/2]$ ,  $[202\ 5/2]$ ,  $[330\ 1/2]$ ,  $[200\ 1/2]$ ,  $[321\ 3/2]$ , and  $[202\ 3/2]$ , from the left [smaller  $(R/r_0)^3$  values] to the right [larger  $(R/r_0)^3$  values] at  $\varepsilon_m \approx 0$ . The neutron numbers 6 and 24, which are obtained by filling in all lower-lying levels, are indicated with circles. We note  $\Omega \equiv m$ .

$$\alpha^2 \equiv -\frac{2m \varepsilon_m}{\hbar^2}. \quad (9)$$

The normalization condition is written as

$$\sum_{\ell j} \int_0^\infty |R_{\ell jm}(r)|^2 dr = 1. \quad (10)$$

For a given value of the deformation parameter  $\beta$  we vary the potential radius  $R$  so as to obtain the required one-particle energy  $\varepsilon_m$ .

In Fig. 1 we show the calculated  $\varepsilon_m$  values, which are relevant to  $s$ - $d$  shell nuclei for the neutron number  $N=6-24$ , for  $\beta=0.5$  as a function of  $R$ . The spherical one-particle levels,  $s_{1/2}$ ,  $d_{3/2}$ ,  $d_{5/2}$ , and  $g_{9/2}$ , are included in the calculation for positive parity, while for negative parity the  $p_{1/2}$ ,  $p_{3/2}$ ,  $f_{5/2}$ , and  $f_{7/2}$  levels are taken into account. Here intentionally we do not write the radial quantum-number  $n$  for the levels included, since the shape of radial wave functions  $R_{\ell jm}(r)$  obtained from Eq. (6) can be very different from that of eigenfunctions of the Woods-Saxon potentials. The structure of deeply bound orbits such as those for  $\varepsilon_m = -10$  MeV is similar to what is expected [3] from the asymptotic quantum numbers in the deformed harmonic-oscillator model. The level energies with  $m^\pi = 1/2^+$ , which are expressed by solid curves with solid circles, are seen to show smaller slope especially as  $\varepsilon_m \rightarrow 0$ , though in this example the order of levels does not happen to change in the limit.

In Fig. 2 the calculated probabilities of the  $s_{1/2}$ ,  $d_{3/2}$ ,  $d_{5/2}$ , and  $g_{9/2}$  components in the  $[220\ 1/2]$  level are shown as a function of  $\varepsilon_m$ . It is observed that the  $s_{1/2}$  component becomes dominant as  $\varepsilon_m \rightarrow 0$ . The  $s_{1/2}$  wave function for small

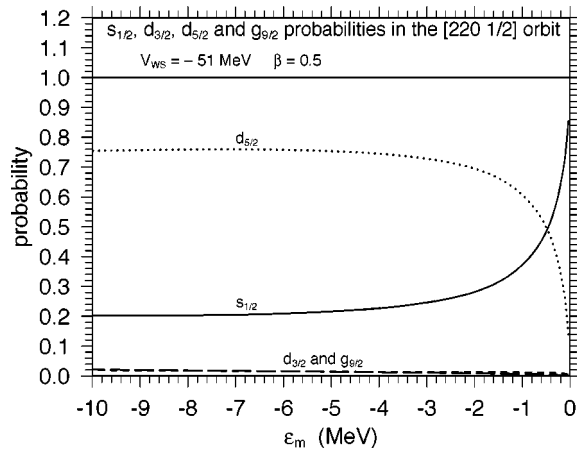


FIG. 2. Calculated probabilities of  $s_{1/2}$ ,  $d_{3/2}$ ,  $d_{5/2}$ , and  $g_{9/2}$  components in the  $[220 1/2]$  level as a function of energy eigenvalue  $\epsilon_m$ .

values of  $|\epsilon_m|$  shows halo structure, and the major part of the large  $s_{1/2}$  probability comes from the outside of the nuclear potential. Since weakly bound  $s_{1/2}$  neutrons are insensitive to the decreasing strength of the potential, the bound  $m^\pi = 1/2^+$  orbits can survive by increasing the  $s_{1/2}$  component. This fact also implies that the major component of any weakly bound  $\Omega^\pi = 1/2^+$  neutrons in deformed nuclei must be  $s_{1/2}$  and thereby show halo phenomena.

In Fig. 3 the probabilities of the  $s_{1/2}$  component in three  $\Omega^\pi = 1/2^+$  Nilsson levels of the  $s$ - $d$  shell,  $[220 1/2]$ ,  $[211 1/2]$  and  $[200 1/2]$ , are plotted as a function of  $\epsilon_m$ . It is seen that in all  $\Omega^\pi = 1/2^+$  orbits the  $s_{1/2}$  component becomes dominant as  $\epsilon_m \rightarrow 0$ . This feature appears for any realistic values of  $\beta$  in deformed nuclei.

What is observed in Figs. 2 and 3 means that in deformed nuclei all Nilsson orbits with  $\Omega^\pi = 1/2^+$  are dominated by the  $s_{1/2}$  component as  $\epsilon_m \rightarrow 0$ , which exhibits halo structure, though the actual value of  $\epsilon_m$  at which the  $s_{1/2}$  component becomes dominant depends on Nilsson orbits. Consequently, those orbits become unavailable for constructing deforma-

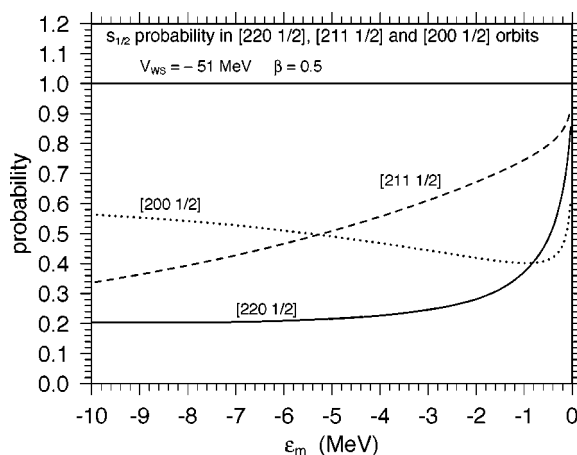


FIG. 3. Calculated probabilities of the  $s_{1/2}$  component in three  $\Omega^\pi = 1/2^+$  Nilsson levels in the  $s$ - $d$  shell,  $[220 1/2]$ ,  $[211 1/2]$ , and  $[200 1/2]$ , as a function of respective energy eigenvalue  $\epsilon_m$ .

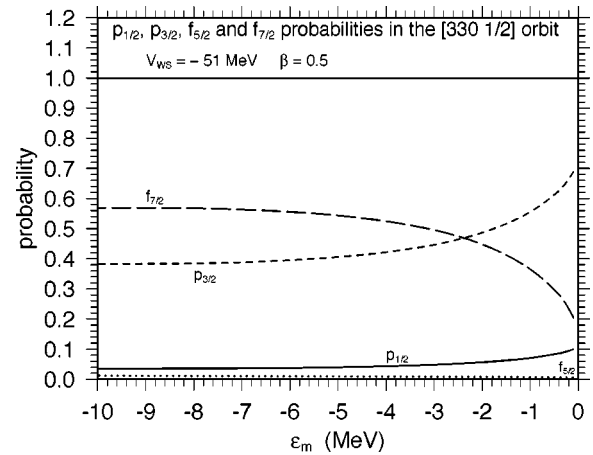


FIG. 4. Calculated probabilities of  $p_{1/2}$ ,  $p_{3/2}$ ,  $f_{5/2}$ , and  $f_{7/2}$  components in the  $[330 1/2]$  level as a function of energy eigenvalue  $\epsilon_m$ .

tion. In Ref. [5] we have found that  $s_{1/2}$  orbits become unavailable for the many-body pair correlation as the energies approach continuum. Combining these findings, we may say that all Nilsson orbits with  $\Omega^\pi = 1/2^+$  become unavailable for both pair correlation and deformation when those orbits approach continuum or lie in the continuum.

What is described above on the  $\Omega^\pi = 1/2^+$  orbits works also, but to a slightly lesser extent, for the  $\Omega^\pi = 1/2^-$  or  $3/2^-$  orbits where the role of the  $\ell=0$  orbit is replaced by that of the  $\ell=1$  orbit. For reference, in Fig. 4 the calculated probabilities of  $p_{1/2}$ ,  $p_{3/2}$ ,  $f_{5/2}$ , and  $f_{7/2}$  components in the  $[330 1/2]$  level are shown as a function of  $\epsilon_m$ . It is observed that the  $p_{3/2}$  component becomes dominant while the probability of the  $f_{7/2}$  component decreases drastically as  $\epsilon_m \rightarrow 0$ . Since a part of the  $\ell=1$  one-particle wave functions remains inside the potential in the limit of  $\epsilon_m \rightarrow 0$ , in contrast to the case of  $\ell=0$  [10], we obtain a milder dominance in the limit. However, since the width of  $\ell=1$  neutron resonant states becomes quickly large as the energies increase in the continuum, due to the low centrifugal barrier [5], all Nilsson orbits with  $\Omega^\pi = 1/2^-$  and  $3/2^-$  become unavailable for both pair correlation and deformation soon after the one-particle energies increase to positive values.

In conclusion, we have shown that the lowest- $\ell$  component becomes dominant in the neutron orbits of the realistic deformed potential as the binding energies approach zero, irrespective of the size of deformation and the kind of orbits. Thus, the structure of the wave functions of weakly bound neutrons is very different from the one expressed by asymptotic quantum numbers in textbooks. All  $\Omega^\pi = 1/2^+$  levels become unavailable for both deformation and many-body pair correlation, as the levels approach continuum or lie in the continuum. Weakly bound  $\Omega^\pi = 1/2^+$  neutrons in deformed nuclei become almost  $s_{1/2}$  neutrons and thereby exhibit halo phenomena. In such a case possible rotational spectra of the deformed halo nuclei must come from that of the deformed core. The properties of weakly bound (or continuum) low- $\ell$  neutrons unique to finite-well potentials should be carefully taken into account when the nuclear structure information is extracted from measured

quantities such as observed neutron emission widths.

The ground-state structure and excitation spectra of the one-neutron halo nucleus  $^{11}\text{Be}$ , which are being studied experimentally at the moment, may be an example directly related to the present result. In the theoretical study of such light halo nuclei various models, which are specific to individual nuclei with adjusted parameters (for example, see Ref. [11]), are often used rather than a mean-field approximation.

However, the mean-field approximation is the simplest general approach to deformed nuclei. Therefore, the physics found in the present work should be useful not only for medium-heavy neutron-rich nuclei but also for gaining a simple intuitive understanding of light halo nuclei.

The author expresses her sincere thanks to Professor Ben Mottelson for fruitful discussions.

- 
- [1] T. Motobayashi *et al.*, Phys. Lett. B **346**, 9 (1995).  
[2] A. Ozawa, T. Kobayashi, T. Suzuki, K. Yoshida, and I. Tanihata, Phys. Rev. Lett. **84**, 5493 (2000).  
[3] A. Bohr and B. R. Mottelson, *Nuclear Structure* (Benjamin, Reading, MA, 1975), Vol. II.  
[4] I. Hamamoto and B. R. Mottelson, C. R. Phys. **4**, 433 (2003).  
[5] I. Hamamoto and B. R. Mottelson, Phys. Rev. C **68**, 034312 (2003); Phys. Rev. C (to be published).  
[6] T. Tamura, Oak Ridge National Laboratory, Report ORNL-4152, 1967 (unpublished).  
[7] A. Bulgac, nucl-th/9907088.  
[8] M. Grasso, N. Sandulescu, Nguyen Van Giai, and R. J. Liotta, Phys. Rev. C **64**, 064321 (2001).  
[9] O. Nathan and S. G. Nilsson, in *Alpha-, Beta-, and Gamma-Ray Spectroscopy*, edited by K. Siegbahn (North-Holland, Amsterdam, 1965), Vol. I, p. 601.  
[10] A. Bohr and B. R. Mottelson, *Nuclear Structure* (Benjamin, Reading, MA, 1969), Vol. I.  
[11] T. Tarutina, I. J. Thompson, and J. A. Tostevin, Nucl. Phys. **A733**, 53 (2004).